Temperature-dependent Auger recombination dynamics in luminescent silicon nanowires

Alex R. Guichard,* Rohan D. Kekatpure, and Mark L. Brongersma†
Department of Materials Science and Engineering, Geballe Laboratory for Advanced Materials, Stanford University, Stanford, California 94305, USA

Theodore I. Kamins
Quantum Science Research, Hewlett-Packard Laboratories, Palo Alto, California 94304, USA
(Received 25 January 2008; revised manuscript received 16 May 2008; published 15 December 2008)

The optical properties of luminescent Ti-catalyzed Si nanowires are analyzed using continuous-wave and time-resolved photoluminescence (PL) spectroscopy at excitation intensities (I_{ex}) above 1 W/cm^2. At these pump intensities, the PL intensity tends to saturate and the PL decay rate decreases with increasing I_{ex}. These results can be described within the construct of a quasi-two-level rate-equation model that allows for exciton-exciton Auger recombination. Analysis shows that the room-temperature Auger coefficient (C_a), and thus, the Auger rate is roughly two orders of magnitude less than those estimated for silicon nanoparticles in an oxide matrix. The temperature dependence of the Auger process in the nanowires resembles bulk Si, in which Auger processes are phonon assisted. This work provides valuable quantitative information on one of the key nonradiative processes limiting optical gain from Si nanostructures and could prove important in the design of a Si-based laser.

DOI: 10.1103/PhysRevB.78.235422 PACS number(s): 78.67.Lt

I. INTRODUCTION

As an indirect band-gap semiconductor, bulk silicon (Si) is an inefficient light emitter relative to its direct-gap counterparts, with photoluminescence (PL) external quantum efficiencies (EQE) reaching 10% in only specially prepared high-quality substrates.[1,2] However, efficient PL has been observed in various nanostructured Si material systems, such as porous Si and Si nanocrystals (Si-nc) within dielectric matrices.[3,4] Internal quantum efficiencies of the radiative process higher than 60% have been measured in some cases.[5] This high efficiency is attributed to the suppression of nonradiative decay pathways, as well as an increase in the radiative decay rate due to quantum confinement. The observation of time-resolved optical gain on nanosecond time scales from silicon-rich oxide films[6] has recently generated much interest in the creation of an electrically pumped all-Si laser.[7] However, the long radiative lifetime in these systems means that short-lifetime nonradiative processes can dominate at high pump powers, thereby, limiting the possibility of continuous-wave optical gain.

A key process reducing optical gain in Si-nc at high carrier injection levels is Auger recombination (AR),[8] whereby excited carriers recombine nonradiatively and transfer the energy to other carriers.[9] Many studies of AR in bulk semiconductors for various dopant concentrations and carrier injection levels (via optical excitation) have been performed, and the Auger process in the bulk is quite well understood both theoretically and experimentally.[10–13] Despite the wealth of knowledge on AR in bulk Si and its prevalence in Si-based light emitters, little experimental work has been done to quantify this process in luminescent Si nanostructures and understand its dependence on the dimensionality of the system.

The size and dimensionality of a semiconductor is known to greatly affect the character and rate of the Auger process. In most bulk semiconductor systems at room temperature, including Si, AR occurs via a process involving three free carriers, and the PL decay rate (the reciprocal lifetime with units s^{-1}) is proportional to the square of the carrier concentration, N^2. In contrast, one-dimensional (1D) structures can exhibit increased electron-hole overlap and dielectric constant mismatch between the host wire and its surroundings. This can result in an exciton binding energy that exceeds the thermal energy, k_BT.[14,15] In this case, the majority of the excited carriers are in the form of excitons and AR occurs in the form of exciton-exciton or so-called *bimolecular* annihilation. Since this process involves two bound electron-hole pairs (or particles), this bimolecular AR rate scales linearly with N. Theoretical and experimental studies of compound semiconductor nanowires (NWs) have shown such linear dependence of the PL decay rate on carrier concentration.[16,17] There are few such studies on confined indirect band-gap systems, and none have experimentally explored this process and its temperature dependence in 1D Si wires.[18]

In this paper, we study the onset of AR in luminescent Ti-catalyzed Si nanowires (SiNWs) by measuring the excitation intensity dependence of the PL and the PL decay lifetime. Our results are well explained by a quasi-two-level model that accounts for excitonic Auger recombination, and this model allows us to deduce a value of the Auger coefficient, which quantifies the propensity for Auger recombination over a range of carrier concentrations. Measuring the Auger coefficient at temperatures ranging from 400 down to 4 K, we show that the Auger rate in NWs is lower than the rate in both Si-nc and bulk Si. This finding is significant for the design of an electrically pumped laser based on Si nanostructures.[7] The temperature dependence of the Auger Coefficient suggests that the AR process occurs via the mediation of phonons—similar to phonon-assisted AR in bulk Si.

 ©2008 The American Physical Society

II. EXPERIMENT

A. Nanowire growth and oxidation

$TiSi_2$-catalyzed SiNW arrays were grown by depositing Ti on an Sb-doped, *n*-type (100)Si wafer. The samples were then annealed at 900 °C in H_2 for 5 min to form the $TiSi_2$ catalyst islands. To grow the NWs, the samples were exposed to a mixture of SiH_4, HCl, and H_2 at 680 °C for 30 min.[19] Judging from the solid solubility of Ti in bulk Si at the growth temperature, the Ti impurity concentration in the SiNW is believed to be on the order of 1×10^8 cm^{-3} and, therefore, will have a negligible effect on the electronic properties.[20] Following NW growth, the samples were etched in 2% HF for 1 min to remove the native oxide from the NWs. The NW samples were then thermally oxidized at 950 °C for 40 min to shrink the nanowire crystalline core diameter to 3.3 ± 1.6 nm.[21] This decrease in diameter induces a shift in the PL energy from its bulk value due to quantum confinement effects. Immediately following oxidation, the samples were annealed in Ar at the oxidation temperature, then annealed in forming gas (5% H_2 and 95% N_2) at 450 °C for 30 min to ensure all oxidants in the wire have reacted with the SiNW core and to passivate defects.

B. Photoluminescence analysis

NW samples were loaded into an Oxford Instruments MicrostatHe liquid He cryostat and pumped to high vacuum (10^{-6}-Torr range). The sample temperature was controlled between 4 and 400 K. The 488-nm line of an Ar^+ ion laser was used to excite PL, focused to a spot area of 0.017 mm^2 on the sample. Using a continuously variable neutral density filter, the excitation intensity was controlled from 0.1 to 100 W/cm^2. The excitation power was measured with an optical power meter, and the excitation spot size was determined at the focal point with the razor edge technique. PL was collected and passed through an Acton grating monochromator, and spectra were measured using a Princeton Instruments liquid nitrogen-cooled Si charge coupled device (CCD) connected to the monochromator. All spectra were corrected for the CCD spectral response. PL lifetime measurements were made by modulating the continuous-wave Ar^+ ion laser beam with an Acousto-Optic Modulator at a 50% duty cycle and a 1–5-ms period. The laser modulation function is a square wave with a rise time of <10 ns, faster than both the excitation and decay processes by a few orders of magnitude. This waveform allows for excitation of the NWs to steady-state conditions. The time-varying PL was collected and detected by a fast (<5 ns response time) Hamamatsu photomultiplier tube (PMT) connected to a Stanford Research Systems multichannel photon counter.

III. RESULTS AND DISCUSSION

A. PL and lifetime data

Figure 1 shows PL spectra taken from a $TiSi_2$-catalyzed SiNW sample after a 40 min oxidation for three different excitation intensities. The peak position at room temperature under low-pump intensity is around 800 nm, consistent with

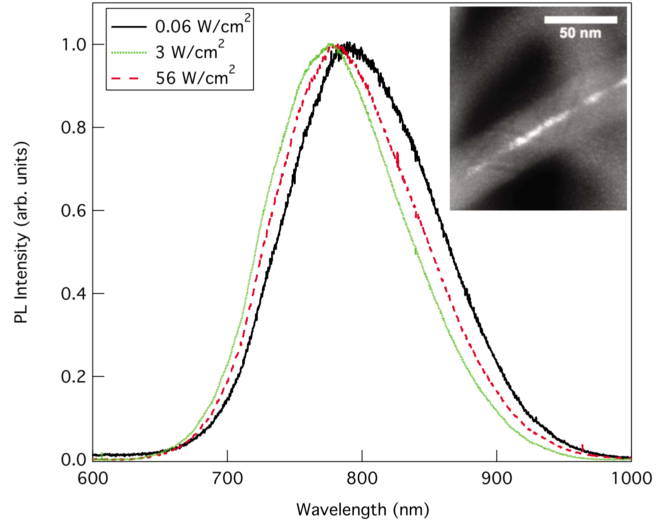

FIG. 1. (Color online) Room-temperature photoluminescence spectra of oxidized Si nanowires taken at pump intensities of 0.06 W/cm^2, 3 W/cm^2, and 56 W/cm^2 (pump wavelength =488 nm). Inset shows representative dark-field transmission electron microscope image of crystalline Si core (bright region) surrounded by an amorphous oxide.

an average SiNW diameter of about 3 nm. The significant width of the spectrum is a direct result of the distribution NW sizes, with the smaller diameter wires emitting at shorter wavelengths.[21] Dark-Field Transmission Electron Microscopy (DFTEM) confirms the presence of crystalline Si cores on the order of 3 nm in diameter (inset). At low excitation intensities ($I_{ex}<0.1$ W/cm^2), the PL decay lifetime (τ_d) at 800 nm (as fit with a stretched exponential decay fit function of the form $\exp[-(t/\tau_d)^\beta]$) is on the order of 50 μs and has a β factor of 0.85. These aspects of the PL suggest it arises from confined excitons in the Si cores.[22–24] Also, it is likely that the multiexponential decay in this system of spatially isolated SiNWs arises from variations in shape and dimension, but could also be related to the indirect gap of the wires.[25–27] An increase in the excitation intensity over three decades induces a small but noticeable 15-nm blueshift in PL peak position (Fig. 1). In Secs. III B and III C, we further investigate the dependence of the optical properties of the NWs on excitation density.

Figure 2 shows the PL intensity and decay lifetime as functions of excitation intensity, I_{ex}. These two quantities exhibit two distinct regimes. At low excitation conditions, the PL intensity scales linearly with I_{ex}, giving rise to a slope of about 1 in the log-log plot. Above 1 W/cm^2, the PL power law becomes sublinear. The decay lifetime is constant at low-pump intensity, but decreases at intensities above a similar threshold. To investigate the lifetime shortening, we compare two PL decay traces taken with high and low I_{ex} (inset). The low-I_{ex} trace taken at 0.19 W/cm^2 is best described with a stretched exponential decay curve with $\beta=0.85$ and a lifetime of 49 μs. The trace taken at 56 W/cm^2 shows a substantial shortening of the $1/e$ lifetime as well as a decrease in β, but retains the long-lifetime behavior. The observed PL saturation and lifetime shortening at high I_{ex} are consistent with and attributed to AR

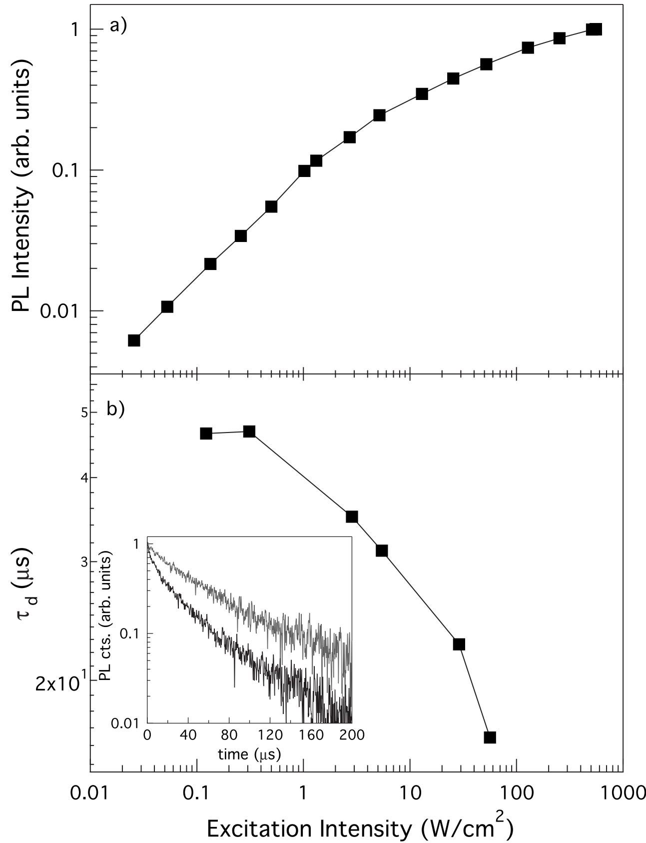

FIG. 2. (a) Log-log plot of photoluminescence (PL) intensity vs excitation intensity for $TiSi_2$-catalyzed Si nanowires. The solid line serves as a guide for the eye. (b) Log-log plot of PL decay lifetime, τ_d, as a function of excitation intensity. The line is a guide for the eye. The horizontal axis range is the same for both plots. The inset shows two normalized PL decay traces, taken at different excitation intensities. The gray line was taken at 0.19 W/cm^2 and the black line was taken at 56 W/cm^2.

effects.[13,18] The observed blueshift with increasing I_{ex} is also consistent with AR recombination setting in at low I_{ex} for the larger diameter (and thus larger excitation cross section) SiNWs.

B. Excitation cross section

In order to provide a quantitative analysis of the Auger process, we need to determine the excited carrier concentration as a function of I_{ex}. To this end, we must first determine the excitation cross section, σ. The excitation cross section can be found by considering the state-filling equations in the low-pump-power regime, where AR can be ignored. The procedure is similar to the one used for Si nanocrystals.[6] The pump-power-dependent PL rise time, τ_{on}^{-1} is given as a function of excitation photon flux, ϕ

$$\tau_{on}^{-1}(\phi) = \sigma\phi + \tau_{d,o}^{-1}. \tag{1}$$

Figure 3 is a plot of room-temperature excitation rate, τ_{on}^{-1}, as a function of excitation photon flux ϕ (equal to $I_{ex}/\hbar\omega$) for low I_{ex} below the Auger threshold. τ_{on} is found by fitting a function of the form $1-\exp(-t/\tau_{on})$ to the lifetime trace

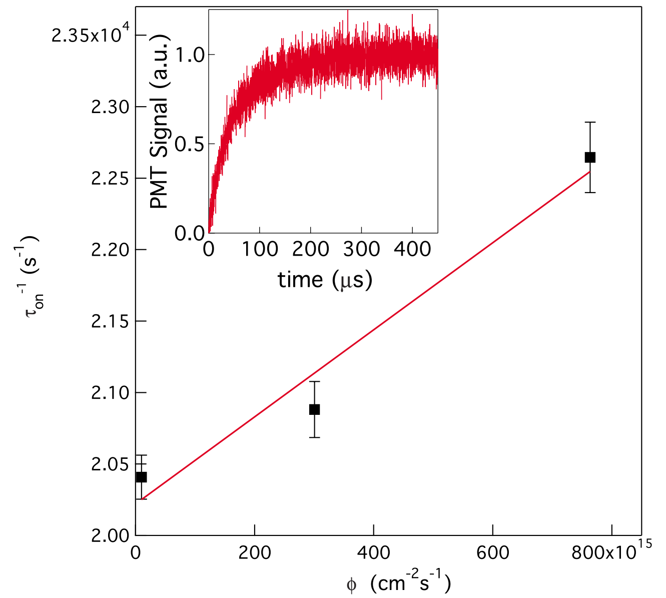

FIG. 3. (Color online) Plot of excitation rate, τ_{on}^{-1} as a function of excitation photon flux, ϕ. Inset shows the PL signal as a function of time during a 488-nm excitation pulse with average power of 0.19 W/cm^2 and period of 1 ms with a 50% duty cycle.

while the excitation laser is on. The slope of the linear fit to the data in Fig. 3 yields σ, and the y intercept is the intrinsic low-I_{ex} decay lifetime, $\tau_{d,o}$.

Using this procedure we find that σ is 3×10^{-15} cm^2 at the excitation wavelength of 488 nm and detection wavelength of 800 nm. This σ is roughly an order of magnitude higher than that measured for Si nanoparticles.[6,28] The increase in excitation cross section cannot simply be attributed to the change in electronic properties with dimensionality because one would expect less absorption for less-confined indirect band-gap geometries. Rather, it is likely that the increase in σ is due to increased optical excitation field strength inside the wire as compared to a spherical geometry. In general, the optical-absorption cross section of a nanoscale object under randomly polarized illumination can be estimated from the expression $\sigma=\alpha V|f|$. Here, V is the object volume, α is the bulk intensity absorption coefficient, and $|f|$ is a factor that accounts for geometry-dependent field enhancement inside the object.[29,30] Using dielectric data for bulk Si, the light intensity enhancement inside a wire is a factor of 5 to 15 greater than that of a spherical particle for silica and air hosts, respectively.[31] This cross section is expected to be relatively temperature independent.[32]

C. Auger coefficient

We are now in a position to quantitatively analyze the AR process by revisiting the decay data in Fig. 2(b). As the decay traces at sufficiently high I_{ex} exhibit two distinct time scales, we can fit those traces with a double exponential function of the form

$$N(t) = A\exp\left[-\frac{t}{\tau_a}\right] + (1-A)\exp\left[-\left(\frac{t}{\tau_{d,o}}\right)^{\beta}\right]. \tag{2}$$

The first term describes the AR process and τ_a is defined as the Auger lifetime. This term dominates at short time scales.

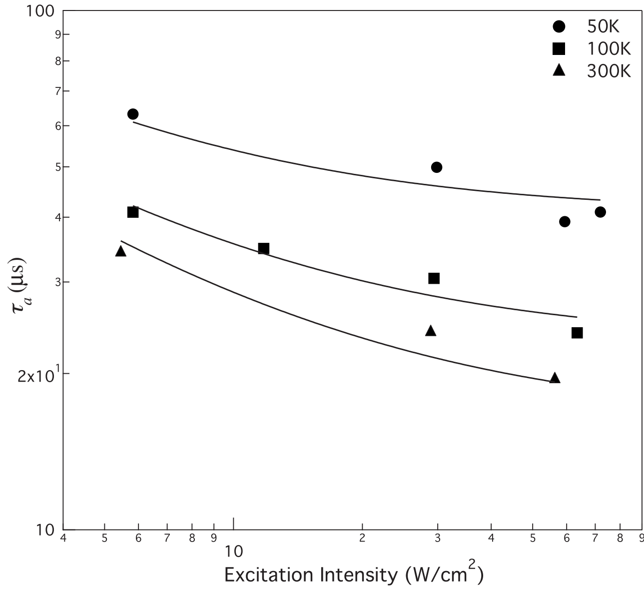

FIG. 4. Plot of Auger lifetime, τ_a, vs excitation intensity at 50, 100, and 300 K. The solid lines are fits using the two-level model shown in Eqs. (3) and (4).

The second term describes the behavior at longer time scales and $\tau_{d,o}$ and β are fixed parameters found from the stretched exponential fitting procedure used in the low-I_{ex} regime. Figure 4 shows the values of τ_a determined as a function of I_{ex} at three different temperatures.

By studying the dependence of τ_a on I_{ex} with a rate-equation model, we determine an Auger coefficient that describes the AR rate at a certain carrier concentration. If we assume that at all temperatures, excited carriers form excitons which can participate in bimolecular AR,[14,33] then the upper-state (i.e., the exciton state) population is described by the differential equation

$$\frac{dN}{dt} = \frac{\sigma I_{ex}}{\hbar\omega}(N_T - N) - \frac{N}{\tau_{d,o}} - C_a N^2, \quad (3)$$

where N_T is the total number of upper and lower states and C_a is the Auger coefficient. In our PL decay experiments, the excitation pulse length was long enough to allow the system to reach steady state at all pump intensities. Since the system was able to reach steady state prior to the decay, the Auger lifetime is dependent on the steady-state concentration just before the excitation pulse is turned off at $t=0$. Therefore, τ_a can be defined as

$$\tau_a = \frac{1}{C_a N_{ss}(I_{ex})}, \quad (4)$$

where $N_{ss}(I_{ex})$ is the steady-state exciton concentration, which is a function of I_{ex}. From our measured τ_a values and the calculated values for N_{ss} at various I_{ex}, we can determine C_a with a least-squares fitting routine. Here, C_a is our only fitting parameter. These fits are shown as the black solid lines in Fig. 4. This analysis yields values for C_a of $(2.1 \pm 0.5) \times 10^{-13}$, $(4.5 \pm 0.15) \times 10^{-13}$, and $(1.3 \pm 0.2) \times 10^{-12}$ cm^3/s at 50, 100, and 300 K, respectively. It is important to note that good agreement is found when modeling the Auger process as a two-particle process. We have also investigated whether our data might be consistent with an Auger process involving three free carriers, such as electron-hole-electron (e-h-e) or electron-hole-hole recombination. This Auger lifetime would scale with $1/N^2$, corresponding to a term that scales with N^3 in a rate equation such as Eq. (3). The best fits for the three-particle Auger process yield trends that are inconsistent with our data. Moreover, the three-particle analysis yields values for C_a that translate to physically unrealistic Auger lifetimes on the order of 1 s. In agreement with previous predictions, the Auger process in these 1D Si wires is indeed a two-particle process involving two excitons and its rate scales linearly with N.

One possible mechanism for lifetime shortening is the local heating of the Si nanostructure at high excitation intensities.[34,35] However, both the PL intensity and Auger lifetime vs excitation intensity trend are the same at all temperatures from 4 to 400 K examined in this study, which excludes the possibility of local heating of the SiNWs from the excitation laser as a possible mechanism for the PL intensity saturation and decay lifetime shortening in this intensity range observed here. At low excitation intensities, the decay lifetime of Si nanostructures increases sharply below 100 K and approaches 1 ms near 4 K.[36] From 100 to 300 K it changes by roughly a factor of 5, much less than the factor of more than 10 change at lower temperatures. Therefore, if heating were an issue in these measurements, the PL decay lifetime would change much more drastically with I_{ex} (or temperature) at 4 K than at 300 K and our model for AR would not fit for all temperatures examined. Moreover, according to Refs. 37 and 38, no significant temperature increase is expected for the excitation intensities used in this study. Thus, PL lifetime shortening and intensity saturation due to sample heating are expected to be negligible.

It is worth pointing out that the decay trace fitting function, Eq. (2), employed in our analysis is an approximation and was designed to properly fit both the short and the long non-single-exponential time behavior and to determine these characteristic time scales (i.e., τ_a and $\tau_{d,o}$). Whereas the solution to Eq. (3) captures the physics of exciton recombination and bimolecular AR processes, it does not take into account processes that may give rise to the non-single-exponential behavior at long time scales. The solution to Eq. (3) after excitation is turned off at $t=0$ is

$$N(t) = \frac{N_{ss}\exp[-t/\tau_{d,o}]}{1 - C_a N_{ss}\tau_{d,o}\exp[-t/\tau_{d,o}] + C_a N_{ss}\tau_{d,o}}. \quad (5)$$

Figure 5 shows the comparison of the experimental data with the phenomenological double exponential fit [Eq. (2)] and the solution to the rate equation [Eq. (5)]. We find that using the Auger coefficient found from Eq. (4) and the temporal response from Eq. (5) faithfully reproduces the decay characteristics of the system. It is noted that at long times, the simulated trace deviates from that found from the double exponential fit of Eq. (2). This is because the "stretched" multiexponential nature of the decay, typical of Si nanostructures, is not captured in this temporal solution of the system and the decay time is thus underestimated at long

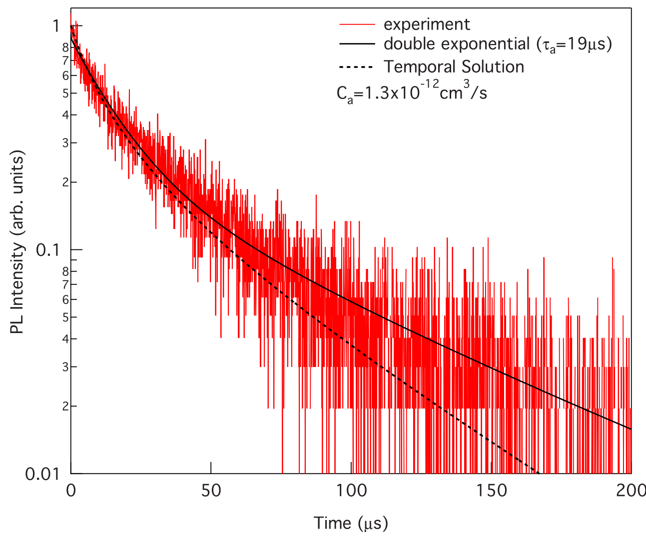

FIG. 5. (Color online) PL decay trace taken at room temperature at 56 W/cm^2. The solid line is a fit using Eq. (2) and the dashed line is the trace predicted from the temporal solution of the model contained in Eq. (5) and the measured Auger coefficient.

times.[25,27,39] Although fitting to a double exponential function [Eq. (2)] is *ad hoc*, it provides good quantitative estimates of τ_a and $\tau_{d,o}$ in the confines of a physically intuitive model, as shown by the accurate modeling of the experimental data by both decay expressions in Fig. 5.

For practical purposes, it is valuable to compare the relative magnitudes of the Auger rates in Si systems of different dimensionality at a fixed, photoexcited electron-hole pair (EHP) concentration. In performing this comparison, it should be kept in mind that the respective mechanisms for AR are distinct and follow different power laws. Consider the Auger coefficient for bulk Si, which is on the order of 3×10^{-31} cm^6/s at room temperature. At a high EHP density of 1×10^{19} cm^{-3}, the AR lifetime $[\tau_a=(C_aN^2)^{-1}$ for three-particle processes] is on the order of 30 ns. This bulk value is of the same order of magnitude that we observe in this nanowire system. At the same EHP density at room temperature, an AR lifetime of about 75 ns is expected for the nanowires in this study. The difference in rate compared to bulk Si should not come as a surprise as both the AR mechanism and band structure are different in the nanowire. It is also of note that our value of τ_a is almost two orders of magnitude longer than that estimated for Si nanoparticles using a rate-equation analysis and fits to nanoparticle PL decay traces.[7] At the same carrier density of 1×10^{19} cm^{-3}, the nanoparticle Auger rate is 1 ns. Since the rate of the Auger transition scales with exciton-exciton wave-function overlap according to Fermi's Golden Rule,[40] a lower Auger coefficient in Si nanowires versus Si nanoparticles can be expected due to the lower degree of quantum confinement in the 1D wire versus the zero-dimensional (0D) dot. This observation is important when one considers the competition of radiative and nonradiative processes in Si nanostructures at high carrier injection levels. Design of the Si nanostructure emitters to influence the strength of Auger recombination could help in attaining higher levels of continuous-wave optical gain.

Figure 6 shows the temperature dependence of the Auger coefficient from 4 to 400 K. It was found that the Auger coefficient decreased by roughly a factor of 20 relative to room temperature to 6.1×10^{-14} cm^3/s at 4 K. At present, a fully developed theoretical model for the temperature dependence of excitonic AR in 1D structures does not exist.[41] However, it is useful to compare our results to the three-particle AR processes seen in bulk semiconductors. The decrease in Auger coefficient at low temperatures is well described by a theoretical model for bulk phonon-assisted AR derived from Fermi's Golden Rule and second-order perturbation theory.[42–45] This model predicts a temperature dependence of the form

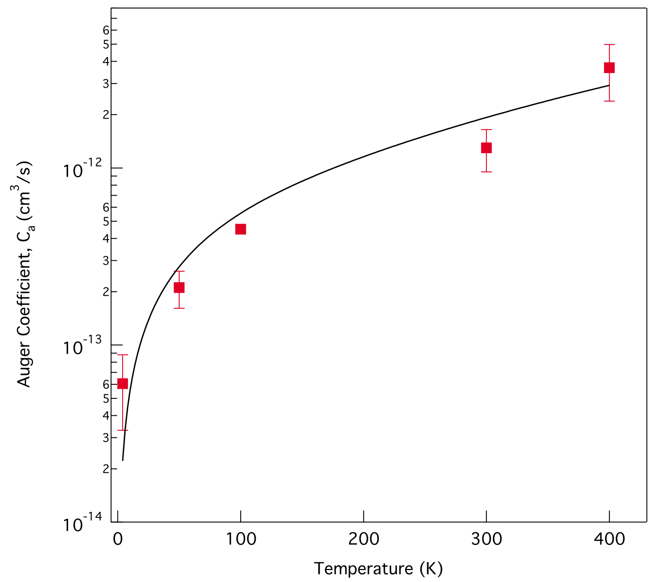

FIG. 6. (Color online) Plot of Auger coefficient versus sample temperature. Solid line is a theoretical fit using the temperature dependence for LO phonon-assisted Auger recombination in a bulk material.

$$C_a(T) \propto \frac{k_BT}{E_{\rm th}^{3/2}}\frac{1}{e^{(E_{\rm LO}/k_BT)}-1}\left(\frac{e^{-E_{\rm th}/k_BT}}{(E_{\rm th}-E_{\rm LO})^2}+\frac{1}{(E_{\rm th}+E_{\rm LO})^2}\right), \tag{6}$$

where $E_{\rm LO}$ is the bulk Si LO phonon energy of 63 meV and $E_{\rm th}$ is the Auger threshold energy. Reasonable agreement is found between this expression and the NW data (see solid line in Fig. 6), and we find that $E_{\rm th}$ is roughly 100 meV, which is larger than the value of 44 meV found for bulk Si.[46] Effects of quantum confinement, Si-SiO_2 interfacial traps and strain in the Si core are not taken into account here and play a role in the discrepancy between Auger threshold energies in wire and bulk. For NWs with diameters of 3 nm, the indirect gap is conserved and phonon-assisted Auger processes are still expected to play a large role.

The results of this study have interesting implications in the realm of Si-based optoelectronics. Recent efforts to demonstrate stimulated emission and lasing in Si nanocrystal systems highlight the important role Auger recombination plays in limiting carrier inversion and possibilities for attaining continuous-wave gain.[6,47] As AR is fast compared to the

spontaneous emission rate at high carrier concentration in indirect-gap semiconductors, careful engineering of both radiative, nonradiative, and AR rates is central to the achievement of an all-Si laser. The Si nanowires in this study have both a larger absorption cross section and a smaller Auger coefficient relative to Si nanocrystals in silica, both of which improve the conditions for achieving continuous-wave gain. From the expression for gain in a two-level system, one can see that the magnitude of the gain is proportional to the degree of population inversion, N_2-N_1, where N_2 and N_1 are the upper- and lower-state populations, respectively.[48] Using Eq. (3) and the measured values of σ, $\tau_{d,o}$, and C_a, we find that the pumping threshold for the onset of population inversion ($N_2-N_1>0$) is roughly three orders of magnitude higher for the nanoparticle system than our nanowire system. Therefore, it is possible that lower threshold lasing could be achieved for a SiNW-based gain medium.

IV. CONCLUSION

Using PL and PL lifetime measurements, we have determined the Auger recombination (AR) coefficient, C_a, and its temperature dependence between 4 and 400 K for $TiSi_2$-catalyzed Si nanowires. The results, interpreted within the framework of a quasi-two-level model, yield Auger recombination lifetimes on the order of 75 ns—two orders of magnitude larger than those for Si nanocrystals at similar carrier densities. The temperature dependence of C_a indicates that the AR process is assisted by phonons, with an energy threshold of 100 meV. The lower values of C_a in SiNWs are important from a fundamental viewpoint and have significant implications for the design of a continuous-wave Si-based laser.

ACKNOWLEDGMENTS

The authors wish to thank Anu Chandran for the useful discussion. This work was funded by the Air Force Office of Scientific Research MURI program, the Global Climate and Energy Project, and by Hewlett-Packard Laboratories.

*guichard@stanford.edu
†brongersma@stanford.edu

[1] T. Trupke, J. Zhao, A. Wang, R. Corkish, and M. A. Green, Appl. Phys. Lett. **82**, 2996 (2003).
[2] E. Yablonovitch and T. Gmitter, Appl. Phys. Lett. **49**, 587 (1986).
[3] L. T. Canham, Appl. Phys. Lett. **57**, 1046 (1990).
[4] K. S. Min, K. V. Shcheglov, C. M. Yang, H. A. Atwater, M. L. Brongersma, and A. Polman, Appl. Phys. Lett. **69**, 2033 (1996).
[5] R. J. Walters, J. Kalkman, A. Polman, H. A. Atwater, and M. J. A. de Dood, Phys. Rev. B **73**, 132302 (2006).
[6] L. Pavesi, L. D. Negro, C. Mazzoleni, G. Franzo, and F. Priolo, Nature (London) **408**, 440 (2000).
[7] L. Pavesi, Proc. SPIE **4997**, 206 (2003).
[8] L. D. Negro, M. Cazzanelli, L. Pavesi, S. Ossicini, D. Pacifici, G. Franzo, F. Priolo, and F. Ia-cona, Appl. Phys. Lett. **82**, 4636 (2003).
[9] S. Sze, *Physics of Semiconductor Devices*, 2nd ed. (Wiley, New York, 1981).
[10] A. R. Beattie and P. T. Landsberg, Proc. R. Soc. London, Ser. A **249**, 16 (1959).
[11] W. Bardyszewski and D. Yevick, J. Appl. Phys. **57**, 4820 (1985).
[12] A. Haug, J. Phys. Chem. Solids **49**, 599 (1988).
[13] J. Dziewior and W. Schmid, Appl. Phys. Lett. **31**, 346 (1977).
[14] M. Bruno, M. Palummo, A. Marini, R. D. Sole, and S. Ossicini, Phys. Rev. Lett. **98**, 036807 (2007).
[15] E. A. Muljarov, E. A. Zhukov, V. S. Dneprovskii, and Y. Masumoto, Phys. Rev. B **62**, 7420 (2000).
[16] I. Robel, B. Bunker, P. Kamat, and M. Kuno, Nano Lett. **6**, 1344 (2006).
[17] H. Htoon, J. A. Hollingsworth, R. Dickerson, and V. I. Klimov, Phys. Rev. Lett. **91**, 227401 (2003).
[18] C. Delerue, M. Lannoo, G. Allan, E. Martin, I. Mihalcescu, J. C. Vial, R. Romestain, F. Muller, and A. Bsiesy, Phys. Rev. Lett. **75**, 2228 (1995).
[19] T. I. Kamins, R. S. Williams, D. P. Basile, T. Hesjedal, and J. S. Harris, J. Appl. Phys. **89**, 1008 (2001).
[20] S. Hocine and D. Mathiot, Mater. Sci. Forum **38-41**, 725 (1989).
[21] A. Guichard, D. Barsic, S. Sharma, T. Kamins, and M. Brongersma, Nano Lett. **6**, 2140 (2006).
[22] D. Kovalev, H. Heckler, M. Ben-Chorin, G. Polisski, M. Schwartzkopff, and F. Koch, Phys. Rev. Lett. **81**, 2803 (1998).
[23] C. Delerue, G. Allan, and M. Lannoo, Phys. Rev. B **48**, 11024 (1993).
[24] M. L. Brongersma, A. Polman, K. S. Min, E. Boer, T. Tambo, and H. A. Atwater, Appl. Phys. Lett. **72**, 2577 (1998).
[25] C. Delerue, G. Allan, C. Reynaud, O. Guillois, G. Ledoux, and F. Huisken, Phys. Rev. B **73**, 235318 (2006).
[26] L. Pavesi and M. Ceschini, Phys. Rev. B **48**, 17625 (1993).
[27] J. Linnros, N. Lalic, A. Galeckas, and V. Grivickas, J. Appl. Phys. **86**, 6128 (1999).
[28] D. Kovalev, J. Diener, H. Heckler, G. Polisski, N. Künzner, and F. Koch, Phys. Rev. B **61**, 4485 (2000).
[29] C. Bohren and D. Huffman, *Absorption and Scattering of Light by Small Particles* (Wiley, New York, 1983).
[30] D. Ricard, M. Ghanassi, and M. C. Schanne-Klein, Opt. Commun. **108**, 311 (1994).
[31] V. I. Klimov, D. W. McBranch, C. A. Leatherdale, and M. G. Bawendi, Phys. Rev. B **60**, 13740 (1999).
[32] D. Kovalev, G. Polisski, M. Ben-Chorin, J. Diener, and F. Koch, J. Appl. Phys. **80**, 5978 (1996).
[33] A. A. Efremov, V. G. Litovchenko, and A. V. Sarikov, Mater. Sci. Eng., C **23**, 165 (2003).
[34] A. G. Cullis, L. T. Canham, and P. D. J. Calcott, J. Appl. Phys. **82**, 909 (1997).
[35] J. C. Vial, A. Bsiesy, F. Gaspard, R. Hérino, M. Ligeon, F. Muller, R. Romestain, and R. M. Macfarlane, Phys. Rev. B **45**, 14171 (1992).

[36] M. L. Brongersma, P. G. Kik, A. Polman, K. S. Min, and H. A. Atwater, Appl. Phys. Lett. **76**, 351 (2000).
[37] H. Scheel, S. Reich, A. C. Ferrari, M. Cantoro, A. Colli, and C. Thomsen, Appl. Phys. Lett. **88**, 233114 (2006).
[38] B. V. Kamenev, H. Grebel, and L. Tsybeskov, Appl. Phys. Lett. **88**, 143117 (2006).
[39] O. Guillois, N. Herlin-Boime, C. Reynaud, G. Ledoux, and F. Huisken, J. Appl. Phys. **95**, 3677 (2004).
[40] W. Lochmann, Phys. Status Solidi A **40**, 285 (1977).
[41] F. Wang, Y. Wu, M. S. Hybertsen, and T. F. Heinz, Phys. Rev. B **73**, 245424 (2006).
[42] V. A. Kharchenko and M. Rosen, J. Lumin. **70**, 158 (1996).
[43] B. K. Ridley, *Quantum Processes in Semiconductors*, 2nd ed. (Clarendon, Oxford, UK, 1988).
[44] W. Lochmann, Phys. Status Solidi A **45**, 423 (1978).
[45] A. S. Polkovnikov and G. G. Zegrya, Phys. Rev. B **58**, 4039 (1998).
[46] L. Huldt, N. G. Nilsson, and K. G. Svantesson, Appl. Phys. Lett. **35**, 776 (1979).
[47] S. G. Cloutier, P. A. Kossyrev, and J. Xu, Nat. Mater **4**, 887 (2005).
[48] P. Bhattacharya, *Semiconductor Optoelectronic Devices*, 2nd ed. (Pearson, Englewood Cliffs, NJ, 1997).